# Effects of Nonlinear Geometric and Material Properties on the Seismic Response of Fluid/Tank Systems

He Liu
University of Alaska Anchorage
Daniel H. Schubert
GV Jones & Associates, Inc.

**Abstract**

Liquid storage tanks are considered essential lifeline structures. Water storage tanks in particular, are important to the continued operation of water distribution systems in the event of earthquakes. Recent earthquakes have shown liquid storage tanks to be vulnerable to damage. Current knowledge about the behavior of liquid storage tanks is extensive, but many of the analytical and theoretical results are for tanks without roof systems, and include a number of simplifying assumptions, for example, small deformation and linear elastic material property assumptions.

To explore the effects large deformation and nonlinear material properties have on the seismic response of fluid/tank systems, the computer program ANSYS was selected to develop a Finite Element Analysis (FEA) model of a ground level, cylindrical steel shell and roof tank structure with contained fluid under seismic load. The ANSYS program was selected for its ability to include shell and structural steel elements, contained fluid elements, fluid-structure interactions, material and geometric nonlinearities, and contact type elements. For purposes of this study, analysis results from a linear elastic, small deformation fixed base model are compared with an elasto-plastic material property model with large deformation assumptions. Results show the significant difference in results based on the assumptions used and indicate that current design code based values may not be conservative in resultant loading calculations.

## Introduction

Recent earthquakes in the US have been moderate in comparison to other parts of the world. Extensive damage and disruption to water and wastewater service have followed most of the major seismic events. Water service was disrupted to 5 million people following the 1985 Mexico City event. 200,000 people were without water service for 1 month following the 1990 Philippine earthquake. By contrast, water service was restored to Northridge California within 4 days (ASCE 1995). Following most major damaging earthquakes, utilities and state governments have responded with renewed interest in methods to mitigate future damage to infrastructure. In areas of large population density and high seismic risk, much emphasis on evaluation and mitigation measures has occurred. In other locations where the risk is not so apparent, preventative measures lag. Many of these are in areas where very large events are possible, but infrequent, resulting in interest in earthquake engineering receiving a low priority.

Alaska has more earthquakes per year than all other states combined. Figure 1 compares the number of seismic events greater than 5.0 (level most likely to be felt) with California. Most are related to the southern coastal areas, with a large proportion of the energy release occurring along the Aleutian chain. The areas of most damage are along the coastal areas and southeast Alaska, but also extending northward into the MatSu Valley and Fairbanks. These areas coincide with the most populated regions of the state. As such, earthquake engineering is an important component in infrastructure design.

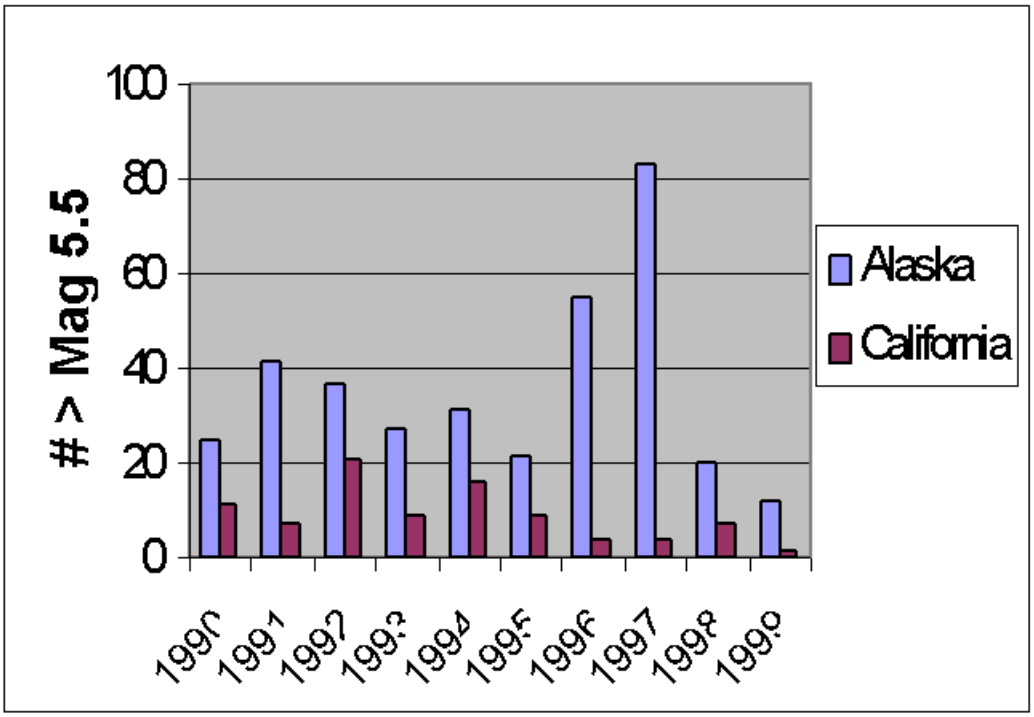


**Figure 1 - Number of Earthquakes in Alaska and California 1990 – 1999**

## Water Storage Tanks

Ground level, cylindrical steel tanks are one of the most commonly used structures for water and fuel storage. Tank design in the United States is based on standards prepared by voluntary committees such as the American Water Works Association (AWWA) or the American Petroleum Institute (API). As important components of community lifeline systems, liquid storage tanks should be designed to survive and continue to function under earthquake events. Damage to tanks and other structures in recent earthquakes, and the prevalence of tanks in areas of high seismic risk has continued interest in their behavior under seismic events (Haroun 1991, Lau 1995). Damage to shell walls and roofs, tear-out of anchors, and pipe connection failures can occur. Due to the damage, the value of the performance of tanks for water supply and fire suppression is significant. The study of the seismic response of liquid storage tanks has been ongoing for the past 40 years. Housner (Housner 1963) and others (Haroun 1991, Veletsos 1984) evaluated the hydrodynamic loading assuming the hydrodynamic response to be divided into two components. The impulsive component included a mass of liquid, which moves in unison with the tank structure. The convective component was associated with the liquid surface wave. Tank analysis was modeled as a single degree of freedom oscillator, with an equivalent mass located at different heights above the base. This allowed determination of the overturning moment and base shear, and still serves as the basis for the AWWA design standards.

### Finite Element Model Approach

Current knowledge about the behavior of liquid storage tanks is still developing. Recent advances and the availability of faster personal computers using structural finite element programs allow for more detailed analysis. The ANSYS finite element program is used for this study. The programs' ability to include contained fluid elements and fluid-structure interactions and other options such as geometric and material nonlinearity such as large deformation assumptions provides many different analysis options. The fluid-tank system selected for detailed analysis is a 500,000 gallon ground level, cylindrical steel water storage tank, located in seismic zone 4. The model of the tank and contained fluid are shown in Figure 2 The properties of the tank are summarized in Table 1.

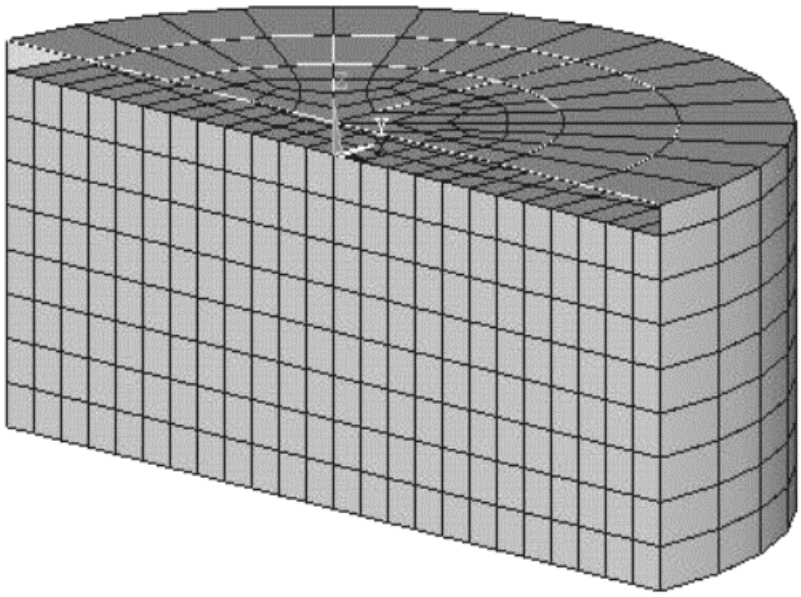

**Figure 2 - Finite Element Tank Model**

**Table 1 - Tank Model Parameters**

| Parameter | | | Parameter | |
|---|---|---|---|---|
| **Geometric Properties** | **Value** | | **Material Properties** | **Value** |
| Height, ft | 24.18 | | Fluid Density, lbm/in$^3$ | 9.35 x 10$^{-5}$ |
| Diameter, ft | 59.42 | | Fluid Bulk Modulus | 30 x 10$^4$ |
| Water Level Height, ft | 22.41 | | Steel Density, lbm/in$^3$ | 7.688 x 10$^{-4}$ |
| Wall thickness, in | 0.1875 | | Steel Poisson Ratio | 0.3 |
| Roof thickness, in | 0.1345 | | Steel Yield Strength, ksi | 36.0 |
| | | | Steel Modulus of Elasticity, ksi | 30 x 10$^3$ |
| | | | Steel Tangent Modulus, ksi | 3 x 10$^3$ |

In the FEA models of this study, the tank roof system is represented by shell and beam elements, which are placed in the radial and circular directions. The tank wall is modeled by shell elements. The contents are represented as contained fluid elements. The fluid elements at the wall boundary are not attached directly to the shell elements but have separate, coincident nodes that are coupled only in the direction normal to the interface. Relative movements in the tangential and vertical directions are allowed to occur. At the base, fluid element nodes are allowed to move on the surface of the tank bottom plate. Due to symmetry, only one half of tank system is modeled.

For this particular contained fluid element, only the lumped mass matrix is available. The Reduced Method is the only acceptable method for modal analyses using these ANSYS fluid elements. The Reduced Method is faster because it uses reduced (condensed) system matrices to calculate the solution. However, it is less accurate because the reduced mass matrix is approximate. The Reduced Method uses the HBI algorithm (Householder-Bisection-Inverse iteration) to calculate the eigenvalues and eigenvectors. It is relatively fast because it works with a small subset of degrees of freedom called Master Degrees of Freedom (DOF). Using Master DOF leads to an exact stiffness matrix [K] but an approximate mass matrix

[M] (usually with some loss in mass). The accuracy of the results, therefore, depends on how well the mass matrix [M] is approximated, which in turn depends on the number and location of masters. The following criteria were used in this study: a) For the fluid elements, master DOF should be at vertical z direction on the surface of the fluid. b) Master DOF were selected at locations having relatively large mass inertia and relatively low stiffness. c) Master DOF were selected in directions in which the fluid/tank system is expected to vibrate. d) Because of the coupled DOF between fluid and tank wall and base, when the degree of freedom to be chosen belongs to a coupled set, only the primary DOF of the coupled set were chosen as masters. e) The total number of master DOF selected should be at least twice the number of modes of interest. A total of 640 master DOF is chosen from the total 10,722 actual number of active DOF of the whole FEA model. From the modal analysis, more than one hundred fluid/tank system natural modes were obtained. It is very important to choose the significant modes from the model analysis results.

## Linear Elastic Small Deformation Analysis Results

### *Modal Analysis Results*

Linear elastic small deformation analysis is performed first for modal analysis. The significant natural modes were chosen starting from the comparison of the participation factors, modal coefficients, and mass distribution percentages for each mode extracted. The participation factors and modal coefficients are calculated based on an assumed unit displacement spectrum in the assumed seismic excitation direction, x-axis in the global Cartesian coordinates. Larger mass distribution percentages usually indicate important modes in the corresponding dynamic response analysis. To ensure the validity of the ANSYS models, modal analyses for fluid sloshing and a combined fluid-tank system was performed. The results were compared with the available theoretical solutions for flexible tanks of fixed support conditions, results of which are summarized in Table 2. The excellent agreements indicate the validity of the ANSYS models. In addition, for the purpose of sensitivity study, the shell wall thickness was varied, from 0.1875 (Tank 1) to 0.2 inch (Tank 2), to compare the effect on the overall response.

**Table 2 - Modal Frequency Comparison**

| | | Wall Thickness (inch) | Natural Period (second) | | | |
|---|---|---|---|---|---|---|
| | | | Horizontal | | Vertical | |
| | | | 1st | 2nd | 1st | 2nd |
| Tank 1 | FEA | 0.1875 | 0.1443 | 0.0810 | 0.1387 | 0.01 |
| | Theory | 0.1875 | 0.1446 | 0.0781 | 0.1498 | |
| Tank 2 | FEA | 0.2 | 0.1398 | 0.0786 | 0.1344 | 0.01 |
| | Theory | 0.2 | 0.1424 | 0.0758 | 0.1451 | |
| Effects of Wall Thickness (Tank 2/Tank 1) | | + 6.67% | - 3.1% | - 2.96% | - 3.1% | 0.0% |

Figure 3 and Figure 4 show the first two horizontal. Figure 5 and Figure 6 show the first two vertical natural mode shapes of the fluid/tank system. These shapes are consistent with the theoretically predicted orthogonal natural mode shapes.

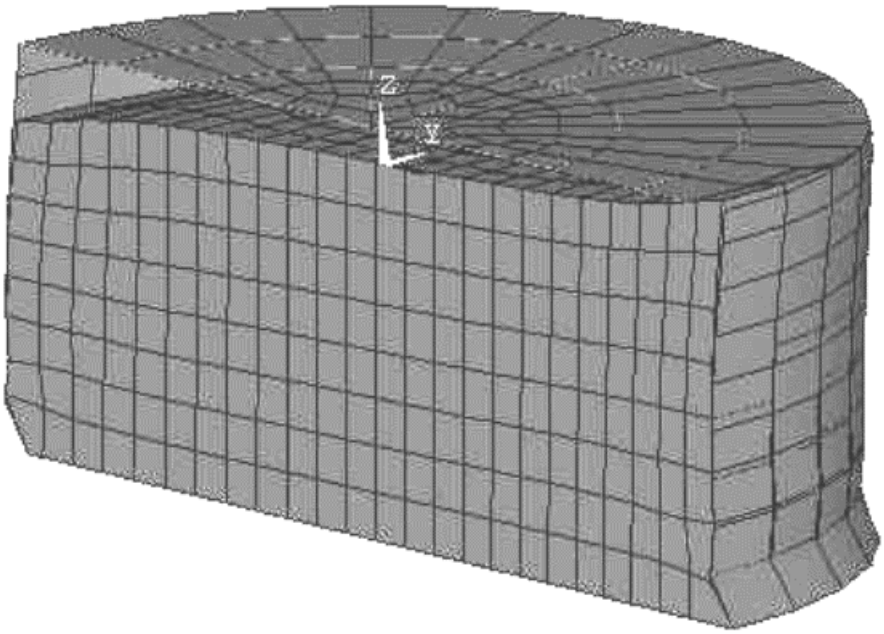


**Figure 3 - The First Horizontal Mode Shape**

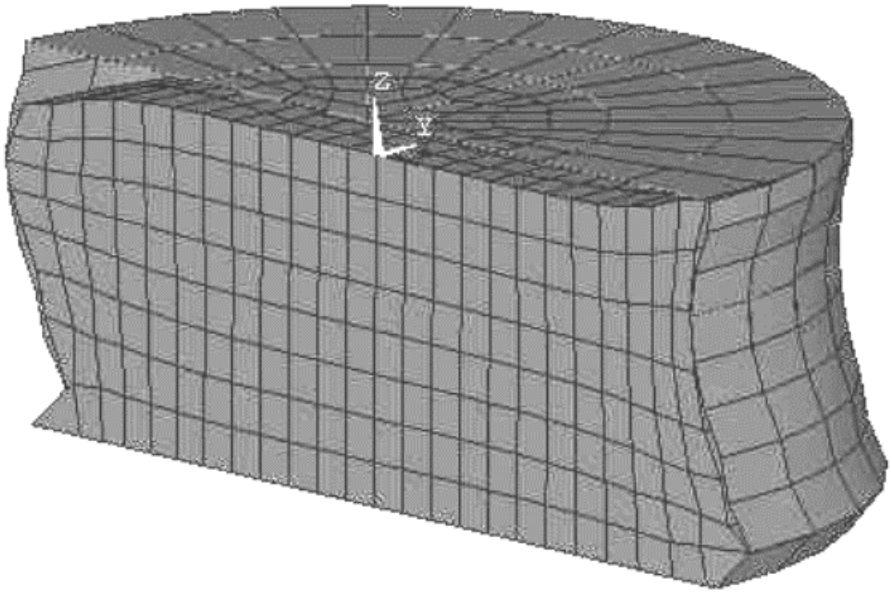


**Figure 4 - The Second Horizontal Mode Shape**

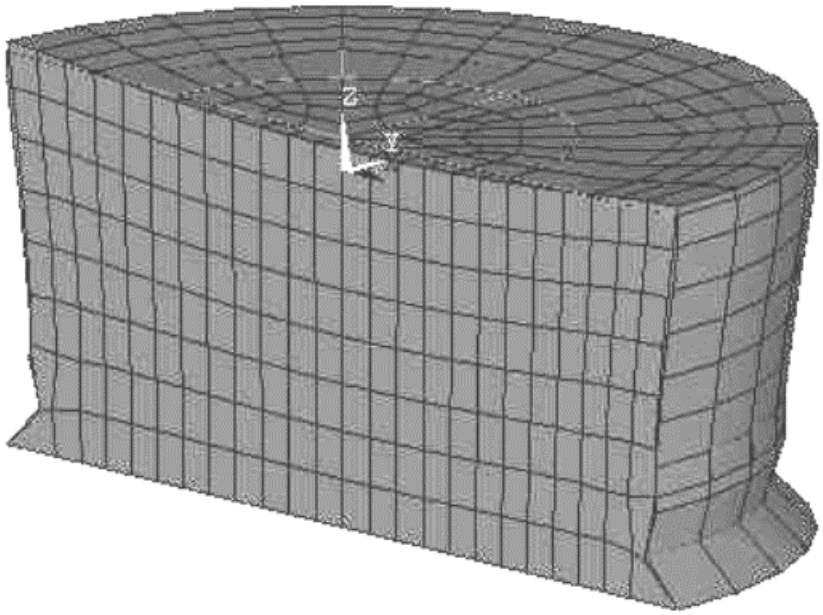

**Figure 5 - The First Vertical Mode Shape**

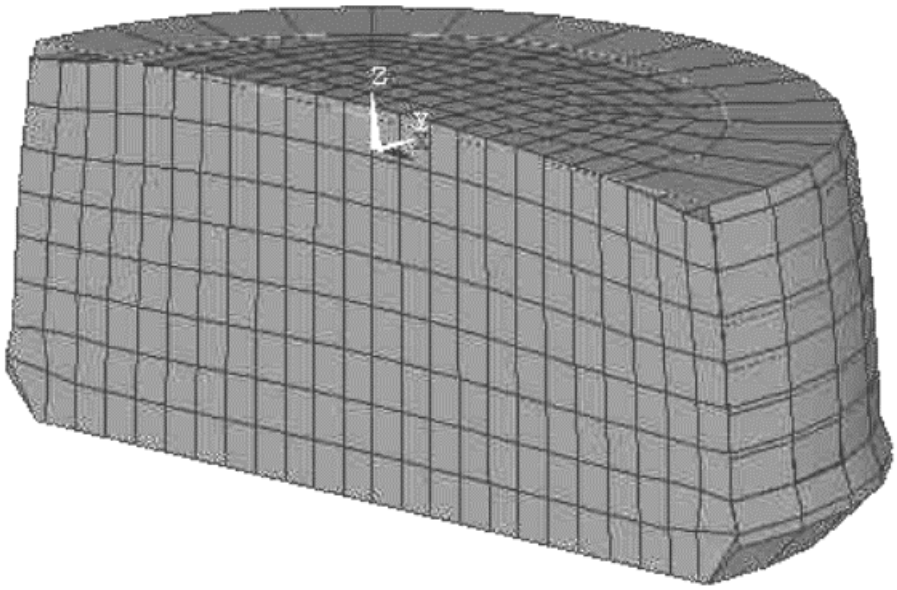

**Figure 6 - The Second Vertical Mode Shape**

## *Time History Analysis and Results*

A time history analysis using the first twelve seconds of the north-south component of the 1940 El Centro earthquake was used for both the linear elastic and the kinematical elasto-plastic model with geometric nonlinearity. Peak ground acceleration values were adjusted to 0.4g. Model time history analysis under linear elastic, small deformation assumptions included evaluation of water surface profiles, base shear, nodal displacements, and resulting stress time history. The following sections summarize results.

## Water Surface Profile

Figure 7 shows the water surface displacement at time of 3.903 seconds. The water surface profile shows distribution of water displacements along the tank centerline in the direction parallel to ground motion, at a maximum vertical displacement time of 3.904 seconds. Figure 8 shows the vertical displacement time history at a point on the upper left water surface. The maximum vertical displacement and time history are almost the same as a rigid tank, which is consistent with theory, and the assumption that the convective effect is almost uncoupled from shell flexibility, impulsive response, and shell motion. The average surface response frequency is close to the first convective mode, implying that the significant hydrodynamic sloshing motion is dominated by the lower convective modes, which also is consistent with theory. The maximum value of vertical surface displacement is on the order of 45 inches, emphasizing the need to provide adequate freeboard to avoid damage to the roof structure. The damage caused by surface waves on roof framing elements and covers has been observed, and supports the usefulness of the model as a predictor of response.

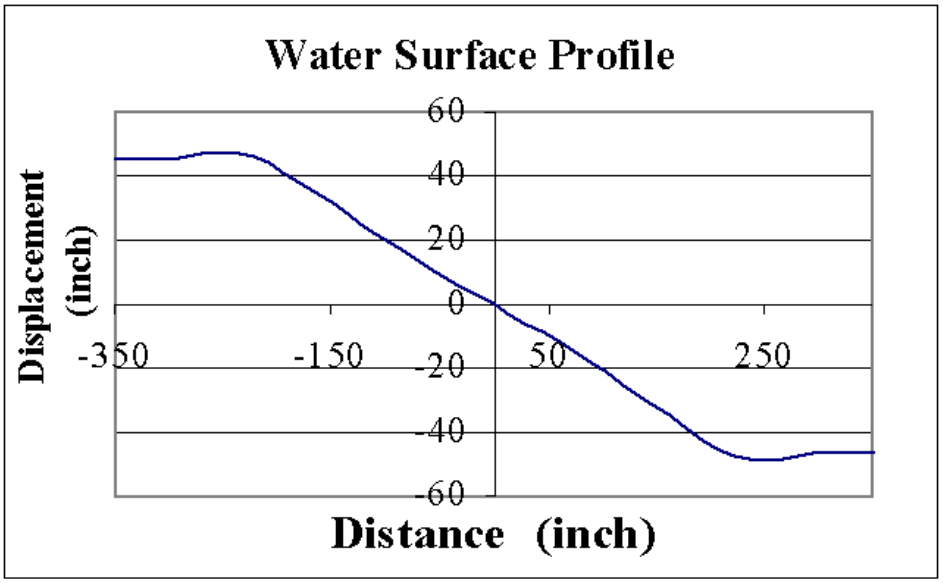


**Figure 7 - Water Surface Profile At Time = 3.903 Seconds**

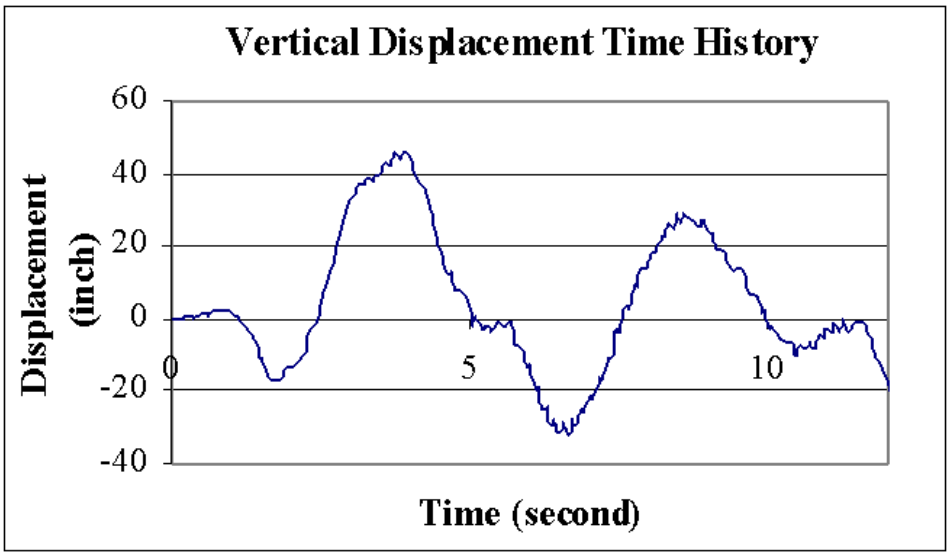


**Figure 8 - Vertical Displacement Time History of a Point at the Upper Left Water Surface**

## Base Shear Time History

Figure 9 summarizes total base shear time history for the fixed base tank with flexible walls. Maximum values of about 8,300 kips occurs at 4.5 seconds. Results are several orders of magnitude larger than values calculated by the AWWA design code, which is expected. Design standards reduce elastic forces by factors of 3 or more to obtain the design forces. Tanks, therefore, respond in a nonlinear fashion when subjected to design ground shaking and experience some damage. In this particular case, the large base shear may also be caused by the frequency sensitivity from the time history combined with the selected tank wall thickness used.

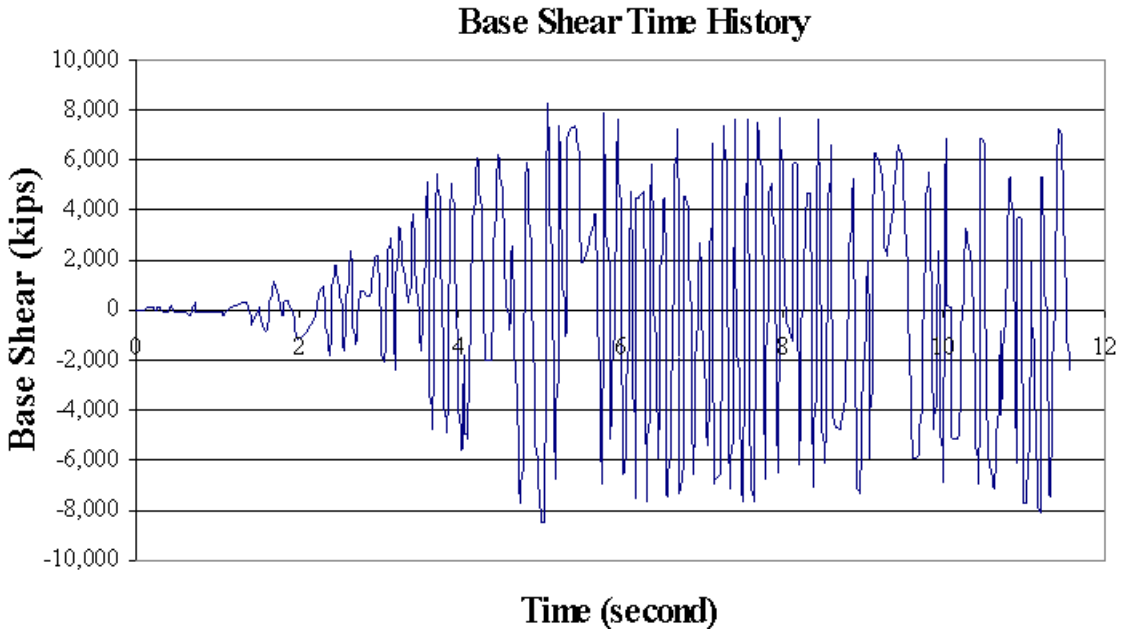


**Figure 9 - Base Shear Time History**

To evaluate the frequency sensitivity effect, the spectrum of El Centro North-south component was studied in further detail. There is a small but very sharp peak in the spectrum near the 0.144 second time period. For the tank under consideration, the first natural period is 0.1443 seconds, with a corresponding effective mass of 97.7%. Thus, the first mode shape dominants the overall horizontal response.

To verify the effect of frequency sensitivity, a second tank "Tank 2" was created with slightly thicker shell wall of 0.20 inch, an increase of 6.67%. The slight increase in wall thickness reduces the first mode period to 0.1398 seconds. The El Centro spectrum is very jumpy around this time period. The base shear time history curve for Tank 2, using the same linear elastic assumptions, shows the change in the shape, frequency content and the peak value. The maximum base shears for Tank 2, is 5,200 kips. Comparing this value with the original tank, Tank 1, shows a peak value decrease in the maximum base shear by about 38%. Such results are indicative of the differences between the resultant time history based analysis and the corresponding spectrum analysis over the code based or smoothed spectrum design approach. In this case, the tank selected for analysis and the corresponding slight change in shell wall thickness can have a dramatic effect on the resulting structural response. This comparison study provides evidence that smoothed spectrum design approach in current practice may not be completely adequate in many cases.

## Elasto-Plastic Large Deformation Time History Results

As previously noted, damage to tanks in past earthquakes in the form of shell wall deformation, and the relatively large base shear results from the model indicate that the simplifying assumptions of small deformation and linear elastic material properties may not be valid. As such, several of the assumptions related to material and geometric linearity were modified to allow a comparison of the results.

## Analysis Assumptions

Because large deformations are expected in this study, large deformation and geometric nonlinearities are applied associated with plastic material response. The elasto-plastic stress-strain curve is assumed for steel wall. Steel exhibits a linear stress-strain relationship up to a stress level of the yield point, 36 ksi in this study. Beyond this point, the stress-strain relationship will become nonlinear and plastic. Several options are available for describing plasticity behavior. The simplest Bilinear Kinematic Hardening option is chosen. It assumes the total stress range is equal to twice the yield stress, so that the Bauschinger effect is included. The plastic behavior is a nonconservative, path-dependent. The sequence in which loads are applied and in which plastic responses occur affects the final solution results. To achieve an accurate solution, in each time step, loads are applied as a series of small incremental sub-load steps, so that the calculation model will follow the load-response path as closely as possible. It is necessary to additionally reduce the load step size after a load step in which a large number of equilibrium iterations was performed.

## Base Shear Time History

Figure 10 shows the base shear time history results for the tank model under the large deformation, bilinear plastic material properties. A maximum value of base shear of 2,900 kips occurs at about 3.5 seconds. As with the linear elastic model, maximum base shear values are larger than those calculated from the AWWA design code.

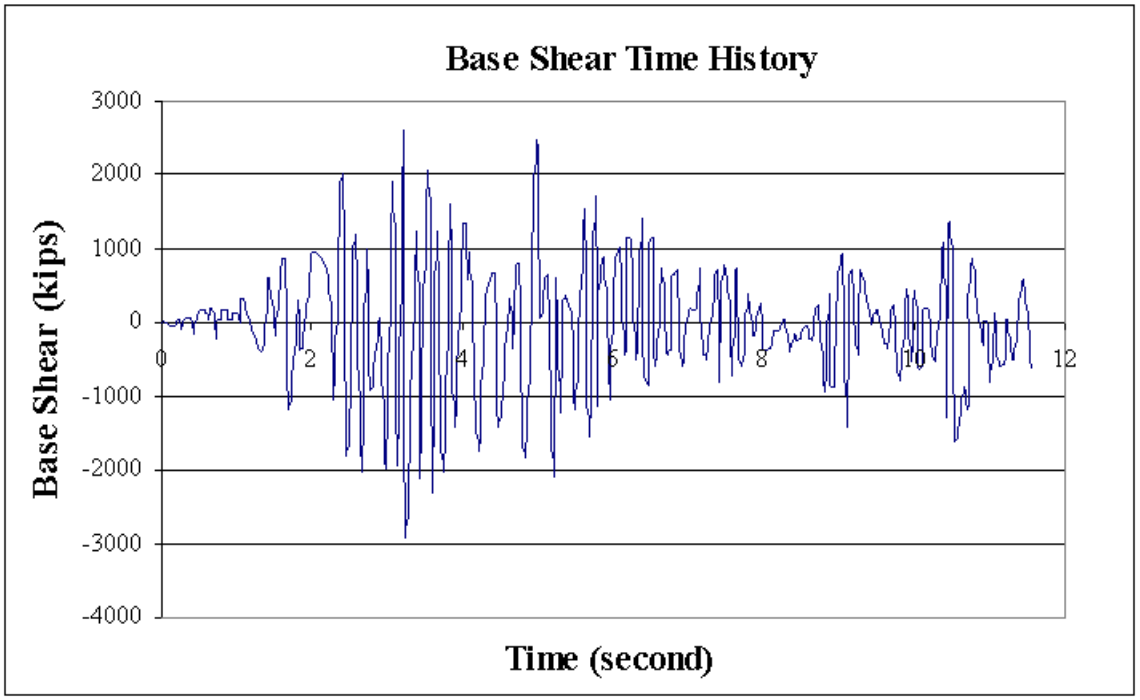


**Figure 10 - Base Shear Time History**

## Large Radial Deformation

Figure 11 shows the results of maximum radial deformation of the shell wall during the time history analysis. This contour is reflective of the maximum inward radial displacement of 8.66 inch at shell wall 58 inch from the top. For comparative purposes, figure 12 is a file photograph showing permanent deformation at the high water level in a water storage tank in California.

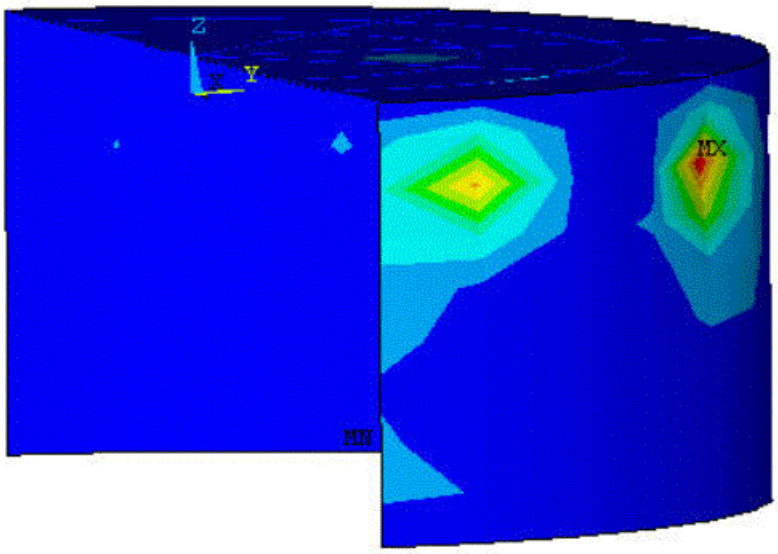


**Figure 11 - Deformation Contour at Time=3.738 Seconds**

**Figure 12 - Tank Samage**

## *Plastic Strain Development*

Figure 13 shows the displacement time history for several nodes located along the periphery of the tank. Node 2935 is located 34-inches from the tank base. Node 2936 is located 58-inches from the top at a horizontal angle of 11.25$^{o}$ measured counterclockwise from right edge of the model, and node 2943 is located at the top at a horizontal angle of 45$^{o}$. These locations correspond to the deformation contour locations shown in Figure 11. The maximum values are -7.66 inches and -8.66 inches respectively for nodes 2936 and 2943. The negative values indicate the inward direction. Figure 14 shows the first principal elastic, plastic, and resultant total strain for a node located at the tank base. Plastic strain initiates

as early as 2.5 seconds after the start of the time history input. As noted, the elastic limit of 36 ksi is reached and permanent deformation is evident.

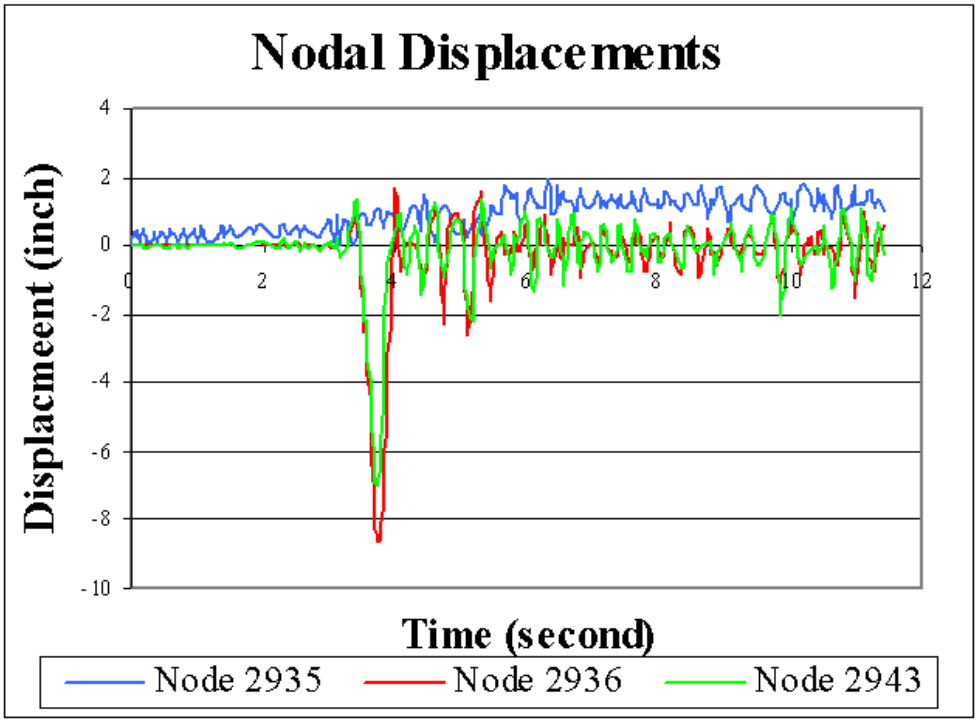


**Figure 13 - Displacement Time History**

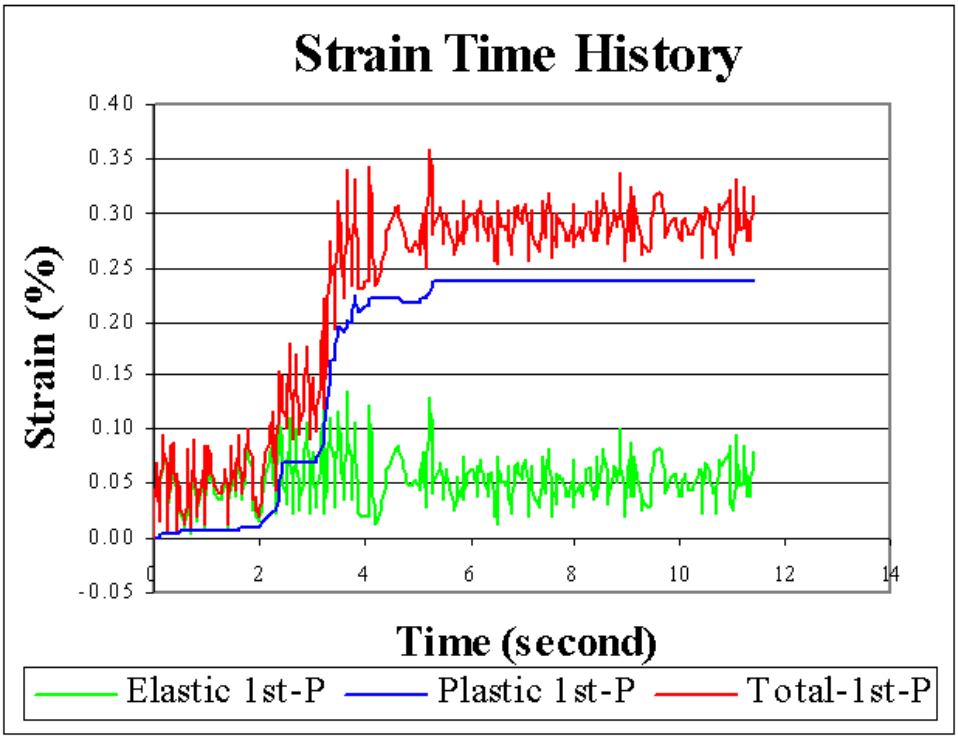


**Figure 14 - Strain Time History**

## *Maximum Pressure Distribution*

Figure 15 shows the contour of water pressure distribution. Figure 16 shows the water pressure distribution at the same time of 3.0 seconds. The vertical pressure distribution is located on the right side of the tank and shows the relative high pressure at a distance about three feet above the base of the tank.

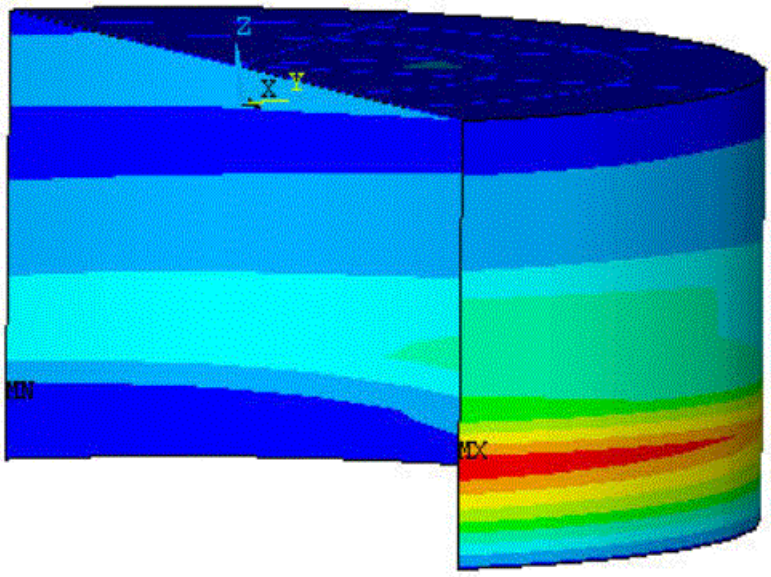


**Figure 15 - Water Pressure Contour at Time = 3.0 Seconds**

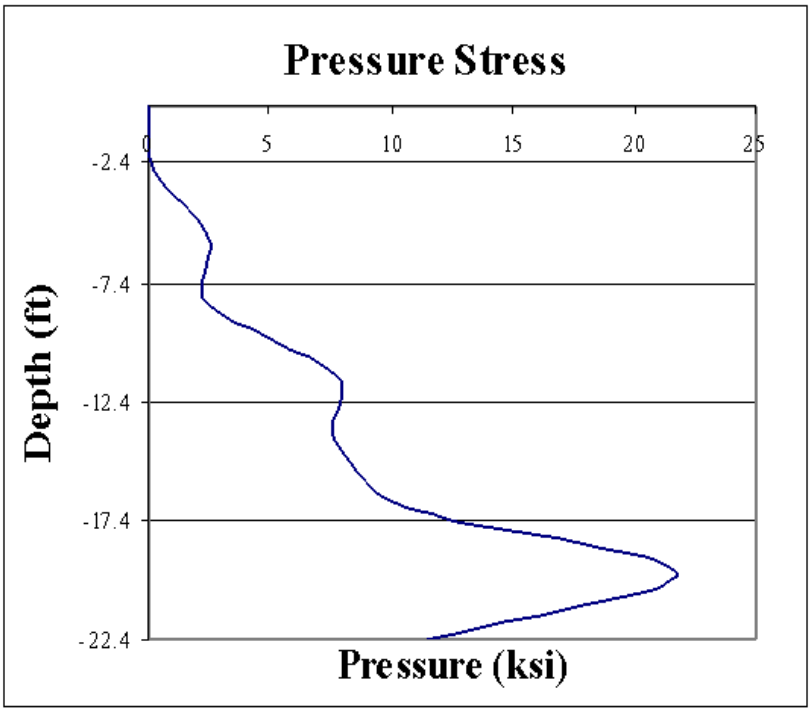


**Figure 16 - Water Pressure Vertical Distribution at Time = 3.0 Seconds**

## *Hoop Stress Distribution*

Figure 17 shows hoop stress contour distribution on the shell wall at time of 3.668 seconds, when the maximum hoop stress of 41.55 kis occurs at the left side of the tank wall. Figure 18 shows hoop stress contour distribution on the shell wall at time of 5.69 seconds, when the maximum hoop stress of 41.1 ksi occurs at the right side of the tank wall. Red (darker) values are higher stress levels, with the blue (lighter) colors representing lower stress levels. The maximum hoop stresses are as high as 41.55 ksi and 41.1 ksi, respectively, which indicate large plastic yield areas near the bottom of the tank.

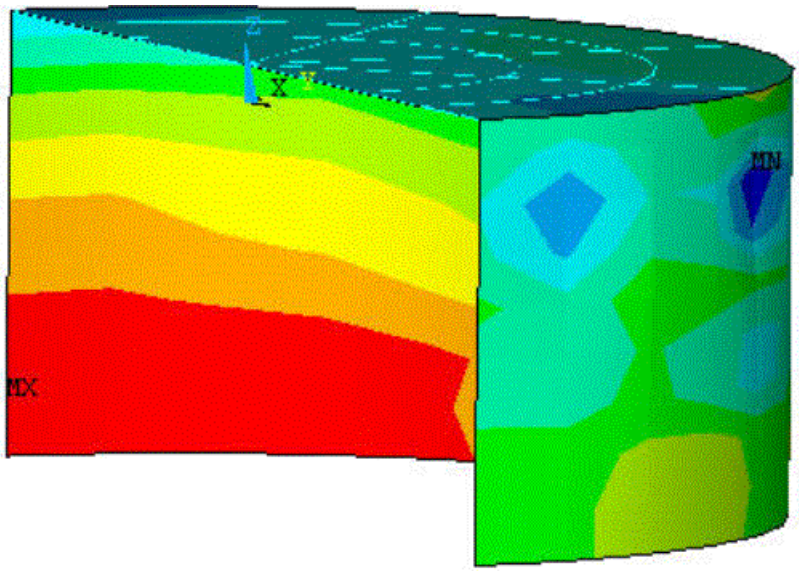


**Figure 17 - Hoop Stress Contour at Time = 3.668 Seconds**

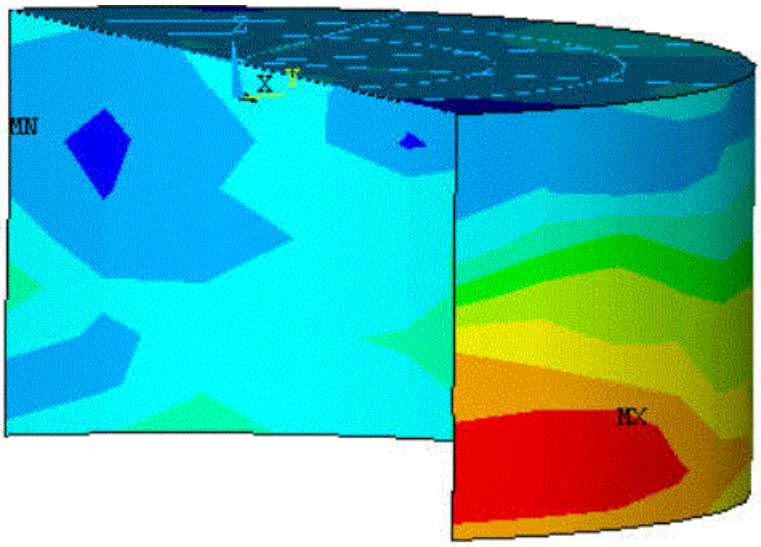


**Figure 18 - Hoop Stress Contour at Time = 5.69 Seconds**

## *Axial Stress Distribution*

Figure 19 shows axial stress contour distribution on the shell wall at time of 3.829 seconds with the maximum tensile stress of 20.66 ksi on the left side of the tank. Figure 20 shows axial stress contour distribution on the shell wall at time of 4.812 seconds with the maximum compressive stress of 18.14 ksi

on the left side of the tank. Red (darker) values are higher stress levels, with the blue (lighter) colors representing lower stress levels.

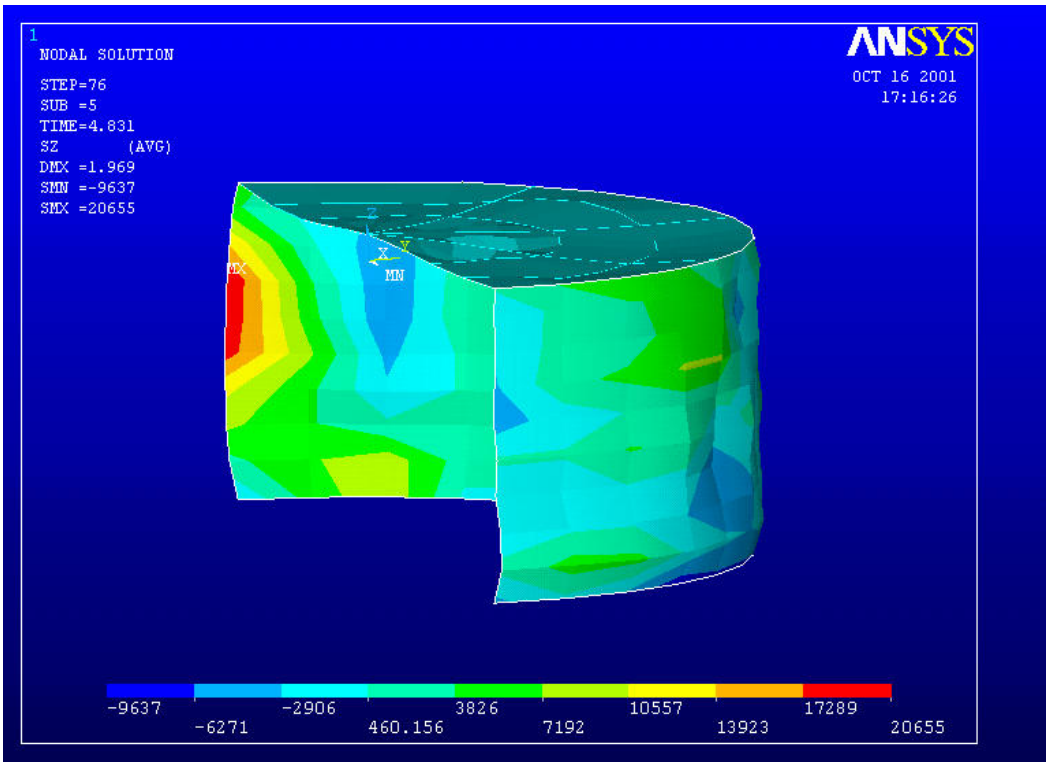


**Figure 19 - Axial Stress Contour at Time = 3.829 econds**

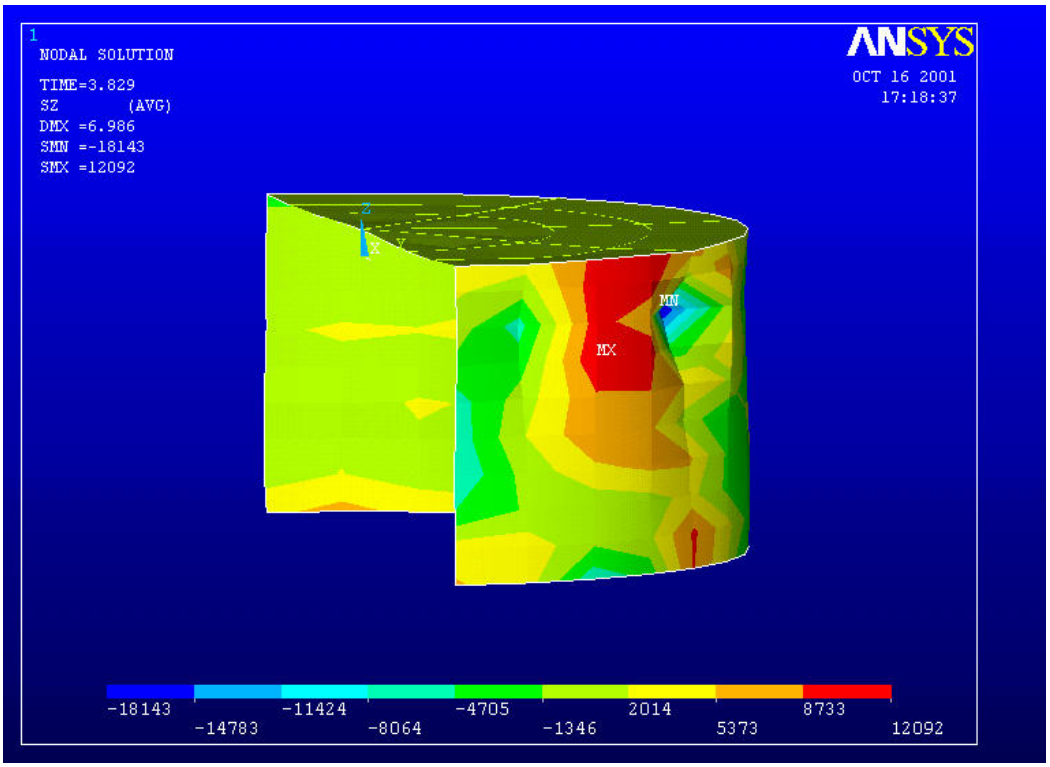


**Figure 20 - Axial Stress Contour at Time = 4.812 Seconds**

## Comparison between Model Results and with AWWA D100

A comparison shows of the time history of water surface profile for the linear elastic model and the elasto-plastic large deformation model are almost identical. Very little difference is apparent in water surface profile, with the exception of greater small scale vibrations in the linear elastic model results after about 3.5 seconds. Figure 21shows a comparison of base shear between the linear elastic and the elasto-plastic nonlinear model. Results show the substantial difference in base shear time history, reflective of the different modeling analysis approach used.

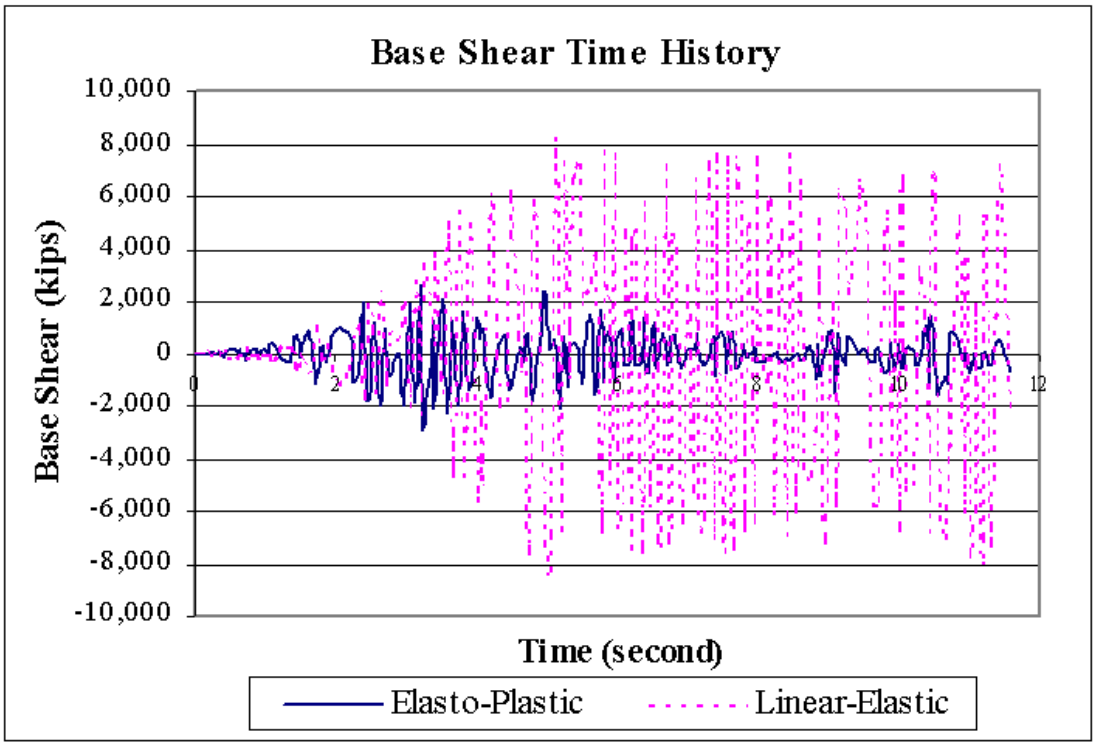


**Figure 21 - Comparison of Base Shear**

## Conclusions

Results of this study show how the assumptions and material properties selected have a large effect on the modeling outputs. In particular, values of displacement, base shear and material stresses show substantial variation. The ratio of base shear between linear elastic and nonlinear properties is about 3.4, which corresponds to the design standard reduction R-factored values of 3.5 for anchored tanks. This indicates that tanks responding in a nonlinear manner when subjected to design ground motions will probably experience structural damage.

Refinements in standard procedures for estimating site-specific earthquake conditions will permit performance based design of tanks and other lifeline structures. Future research will also permit a greater understanding of the response of structures under various seismic loadings, and permit resources to be directed to ensure that functions continue after large earthquake events.

## References


1. ASCE Technical Council on Lifeline Earthquake Engineering, Monograph No. 7, "Critical Issues and State-of-the-Art in Lifeline Earthquake Engineering", ASCE October 1995.
2. "AWWA Standard for Welded Steel Tanks for Water Storage D100-96", American Water Works Association, Colorado.
3. Haroun, M. A., "Implications of Observed Earthquake-induced Damage on Seismic Codes and Standards of Tanks", PVP – Vol 223 Fluid-structure Vibration and Sloshing, ASME 1991.

4. Housner, G.W., (1963) "The Dynamic Behavior of Water Tanks", Bulletin of Seismological Society of America, 53(2) 381-387, Feb.

5. Lau, D. T, Tang, A., and Pierre, J., (1995) "Performance of Lifelines During the 1994 Northridge Earthquake", Can. Jour of Civil Engr 22, 438-451.

6. Malhotra, P., "Practical Nonlinear Seismic Analysis of Tanks", Earthquake Spectra, 16,2, May 2000, 473-492.

7. Veletsos, A. S., (1984) "Seismic Response and Design of Liquid Storage Tanks", in Guidelines for the Seismic Design of Oil and Gas Pipeline Systems, ASCE, 255-370, 443-460.

8. Wozniak, R.S., and Mitchell, W.W., "Basis of Seismic Design Provisions for Welded Steel Oil Storage Tanks", Proc. Refining Dept, Wash. D.C., API 57:485-501.